

# Space Charge Distribution in a Dielectric Liquid Using an Optical Method

Haruo Ihori<sup>a\*</sup>, Hayato Nakao<sup>a</sup>, Masaki Takemura<sup>a</sup>, Mitsuru Oka<sup>a</sup>, Hyeon-Gu Jeon<sup>a</sup>, Masaharu Fujii<sup>a</sup>

<sup>a</sup>A Graduate School of Engineering, Ehime University, 3 Bunkyo, Matsuyama, Ehime 790-8577 JAPAN

\*Corresponding author: ihori@eng.ehime-u.ac.jp

## Article history

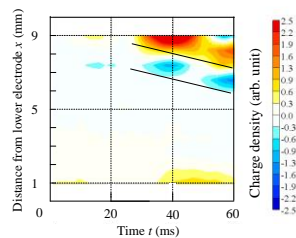
Received :15 February 2013

Received in revised form :

10 June 2013

Accepted :16 July 2013

## Graphical abstract



Temporal change of space charge density map

## Abstract

In order to diagnose the effectiveness of electrical insulation, it is necessary to obtain information regarding the electric field distribution in insulating materials. We have investigated the measurement of electric field vector distributions in liquid dielectrics using an original method. Electric field distributions could be measured in time intervals of milli-seconds by an optical system. In this study, the electric field in a liquid containing space charges was measured, and the change in the electric field caused by the charges in the liquid was examined. Moreover, the space charge distribution in the liquid was also studied. We believe that our study can aid a better understanding of the movement of charges in liquid dielectrics.

**Keywords:** Space charge; Dielectric liquid; Kerr effect

© 2013 Penerbit UTM Press. All rights reserved.

## 1.0 INTRODUCTION

Since dielectric liquids function as both insulators and coolants, they have been widely used in high voltage equipment. In dielectric liquids subjected to a high electric field, space charges are generated due to various reasons, for example, by injection of charges from electrodes or by ionization of the impurities and molecules due to the injection. It is well known that the electric field strength in liquids containing such space charges is not static. It is necessary to obtain information regarding the electric field and space charge distributions in insulating materials to ensure effective insulation. Since it is very difficult to obtain information regarding space charge, particularly in liquids, the electric field in such cases can not be calculated from Poisson's equation as a conventional manner. Therefore, several studies have focused on the direct measurement of electric fields in liquids. The method using the Kerr effect is considered a useful method by which electric fields can be measured without disturbing them.<sup>1-5</sup>

We have previously investigated the three dimensional electric field vector distributions in liquid dielectrics using the Kerr electrooptic effect and a reconstruction technique modified by computed tomography, and symmetrical and nonsymmetrical nonuniform electric field distributions have been measured.<sup>6-7</sup> Recently, the time series analysis of electric field distribution in the order of milli-seconds has been made possible due to significant improvements in the measurement system.<sup>8</sup>

If the time series analysis of the electric field distribution in the gap of a parallel plate electrode system can be obtained, it has been speculated that the time variation of the space charge density distribution can also be obtained from Poisson's equation.

In this paper, we report the measurement of the electric field distribution in a dielectric liquid containing space charges. When a voltage pulse with a long pulse width was applied to a parallel plate electrode system, space charges were generated in the liquid. In our study, we particularly focused on the influence of space charges on the electric field distribution. After a fixed period of time subsequent to the application of the voltage pulse to the electrode system, we measured the electric field distribution upon a second application of the voltage pulse. In this case, the remnant electric charges may be contained in liquid. From the measured electric field distribution, we evaluated electrical conduction in the liquid.

## 2.0 EXPERIMENTAL

The optical measurement system used in our study is shown in Figure 1. We used a He-Ne laser (632.8 nm, 5 mW) as a light source. The laser beam was expanded along the vertical direction to a beam with dimensions of 1.0 cm length and 1.5 mm width; using two cylindrical lenses with different focal lengths. The beam was transmitted through a polarizer, a quarter-wave plate, and a test cell. The test cell was made of synthetic quartz in order to allow the laser beam to pass through. We poured propylene carbonate into

the test cell, as the dielectric liquid sample ( $C_4H_6O_3$ , permittivity 63, viscosity 2.3 mPa, Kerr constant  $1.47 \times 10^{-12}$  m/V<sup>2</sup>).

The beam exiting the test cell was polarized by an analyzer. The intensity of the light exiting the analyzer was measured by an image sensor that had photodiodes arranged at spacing intervals of 0.8 mm. The signal of the image sensor was converted from an analog to a digital signal by the data processing unit, and transferred to a personal computer.

The parallel plate electrode system which was set up in the test cell had circular plates made of brass (with each plate having a diameter of 70 mm and a thickness of 8 mm) as the upper and the lower electrodes. The lower plate electrode was grounded. The gap length was 10 mm. The center axis of the electrode system was irradiated by the expanded laser beam. The electric field strength could be measured every 0.8 mm along the vertical direction via the photo detector.

Initially, when a voltage pulse with a width of 800 ms and amplitude of -10 kV was applied to the electrode system, the change in the optical light intensity was measured at each designated position. The measurements were carried out every 1 ms to 60 ms. We called this measurement the "first sequence".

Next, the voltage pulse was again applied to the electrodes, after an interval of  $T_s$  minutes from the first sequence. The interval  $T_s$  was denoted as the "rest time". The applied voltage pulse for the second sequence was of width 200 ms and amplitude of -10 kV. In this case, the change in the light intensity was measured immediately after the leading edge of the applied voltage.

From the obtained light intensity data, we calculated the electric field strength using the principle of the Kerr electrooptic method.

Starting part of the shape of the applied voltage pulse in the first sequence is shown in Figure 2. Compared with the voltage pulse output by an applied voltage source, the voltage in the gap showed a decrease of about 2 kV during 60 ms. This indicates that an electric current flowed through the electrodes.

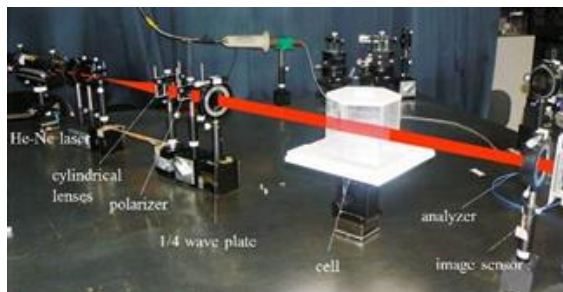


Figure 1 Optical system for measurements

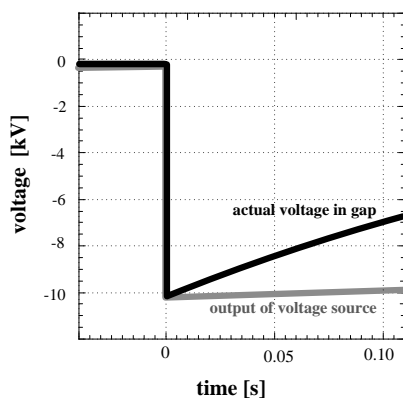


Figure 2 Starting of shape of applied voltage for first sequence

### 3.0 RESULTS AND DISCUSSION

Figure 3 shows the electric field distribution measured during the first sequence. The abscissa indicates the distance from the lower electrode. The absolute value of electric field strength,  $|E|$ , was plotted along the ordinate. The term  $t$  indicates the time elapsed since the applied voltage was started. The time when the voltage pulse rose to its full value was designated as  $t = 0$  ms. The electric field strength  $E$  every 20 ms was plotted in Figure 3. The fitting curves shown in the figure were calculated using the interpolation operator of a graph software.

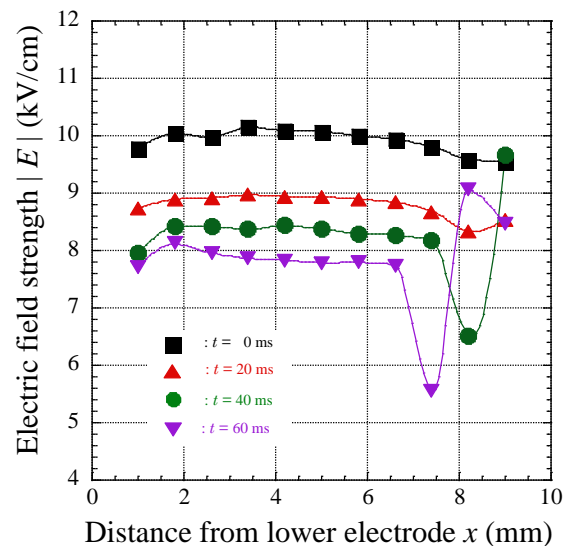


Figure 3 Time series analysis of electric field strength between the gap at first sequence

With increasing values of  $t$ , the electric field strength reduced because the applied voltage was small with time, as shown in Figure 2. At  $t = 0$  ms, the electric field strength was nearly 10 kV/cm; this value was equal to the static field strength calculated theoretically. At certain measured positions near the upper and the lower electrodes, the field strength was slightly less than those at the positions around the center. However, the electric field could practically be considered to be nearly static. For  $t = 20, 40, 60$  ms, the electric field strength showed similar tendencies to that at  $t = 0$  ms for the distances from the center to the lower electrode; however, the absolute field value was less than that at  $t = 0$  ms. In contrast, at the positions near the upper electrode, the electric field strength changed drastically. At these positions, the field strength values were clearly less than the strength of the static field. Moreover, it appeared that the position, at which the field strength was least, shifted towards the lower electrode with increasing values of  $t$ . We speculated that a layer of space charges may have formed in this position and that the layer might have a certain charge density gradient. The layer might move towards the lower electrode or increase over time.

If, we considered that the Poisson's equation

$$\epsilon \frac{dE(x)}{dx} = \frac{\rho(x)}{\epsilon} \quad (1)$$

can roughly approximate the field strength in this case, the differential of  $E$  would be proportional to the space charge density. Therefore, we calculated the differential field strength  $dE(x)/dx$  using the difference method. Figure 4 shows the time variation of  $dE(x)/dx$ , i.e., space charge distribution in the gap.

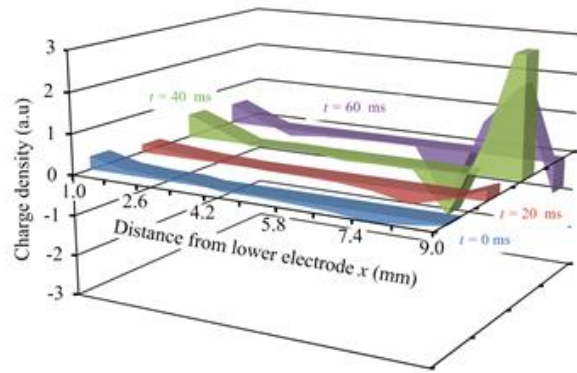


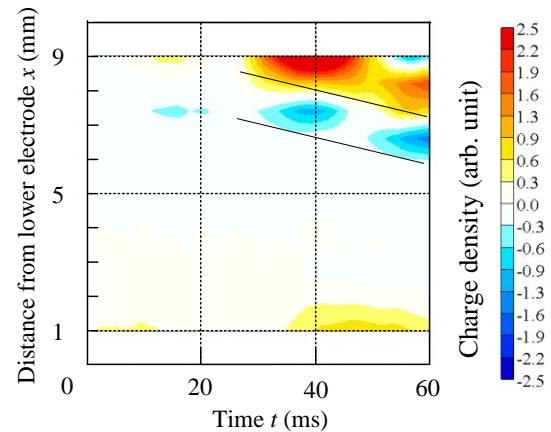
**Figure 4** Time variation of space charge density distribution between the gap

At  $t = 0$  ms, there was no space charge because of the static field. However, we speculated that the space charge existed on the surfaces of the upper and the lower electrodes because the electric field strength near both of these electrodes was less than the static field. According to Poisson's equation, in general, the existence of a charge layer should increase or reduce the electric field strength. For example, in the case of homo charges, the electric field strength was less than the static value. If the measurement had been carried out in the immediate vicinity of the electrodes, more useful information could have been obtained.

At  $t = 60$  ms, a set of negative (homo) - positive (hetero) - negative (homo) charge layers appeared near the upper electrode. At  $t = 20$  ms and  $t = 40$  ms, the negative layer of this set of charge layers that was nearest to the upper electrode was not detected; however, we speculated that a similar set of the layers would exist. It appeared that this set of layers moved towards the anode as  $t$  increased. The negative and the positive charge layers were generated by dissociation or ionization of the impurities and molecules in the liquid. The negative layer moved towards the lower electrode due to the electric field, and the positive layer moved towards the upper electrode. Because another negative layer, which might have been generated by the charges injected from the upper electrode, also moved towards the lower electrode, some of the negative charges were cancelled by some of the positive charges; as a result, the positive layer appeared to move towards the lower electrode.

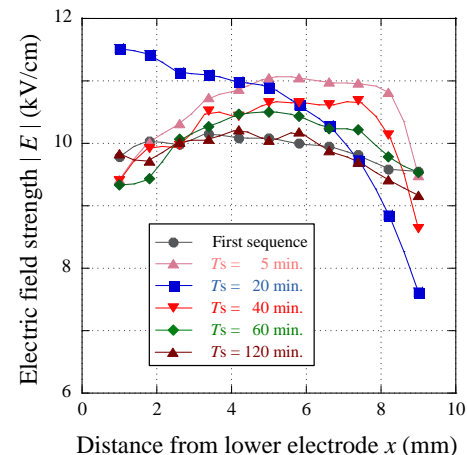
Near the lower electrode, there was no appreciable change in field strength. However, we speculate that abovementioned phenomena (with opposite polarity) also occurred at the upper electrode although the change in the field strength was very small. The validation of our hypothesis would require more experiments under varied experimental conditions, for example, variations in the pulse width, strength, and polarity of the applied voltage.

Figure 5 shows the temporal change of space charge density distribution between the gap at intervals of 1 ms. From the slope of the front of the layer (thin lines shown in Figure 5), the mobility of carriers was determined to be  $4.1 \times 10^{-4}$  ( $\text{cm}^2 / \text{V} \cdot \text{s}$ ). This value would be close to the carrier mobility of ions in common dielectric liquids. This suggests that carrier mobility could be determined by this measurement.



**Figure 5** Temporal change of space charge density between the gap

Figure 6 shows the electric field strength during the second sequence. The rest time  $T_s$  was 5, 20, 40, 60, and 120 min. The plot for the first sequence was the same as that for  $t = 0$  ms in Figure 3. At  $T_s = 5$  min, the absolute value of the electric field strength was very small at the positions near the upper and the lower electrodes. At the positions around the center of the gap, the strength was greater than the static field value of 10 kV/cm. At  $T_s = 20$  min, the electric field strength gradually reduced from the lower electrode to the upper electrode. At  $T_s = 40$  min, the distribution resembled that at  $T_s = 5$  min. Upon increasing the value of  $T_s$ , the distribution approached that of the first sequence. At  $T_s = 120$  min, the electric field strength distribution was nearly identical to that of the first sequence.



**Figure 6** Electric field strength for second sequence

Figure 7 shows the difference quotient calculated from the electric field distribution shown in Figure 6. In the case of the first sequence, the space charge was not detected immediately after initiating the voltage pulse (i.e.,  $t = 0$ ), as shown in Figure 4 or 5. However, as observed from Figure 7, the space charges appeared in the gap, when a measurement was obtained immediately after the application of the voltage. This indicates that the charges generated by the first sequence remained till the initiation of the second sequence, as remanent charges. At  $T_s = 5$  min, we speculated that the layers of the positive charges were formed around the lower electrode and the negative charges were formed around the upper electrode. At  $T_s = 20$  min, the positive charge layer of the lower electrode may have disappeared and negative charges might exist in the gap, particularly, near the upper electrode. During the rest

time  $T_s$ , the charge may have gradually dissipated through the upper and the lower electrodes. For a large value of  $T_s$ , for example,  $T_s = 120$  min, most of the remnant charge would be dissipated before the second sequence.

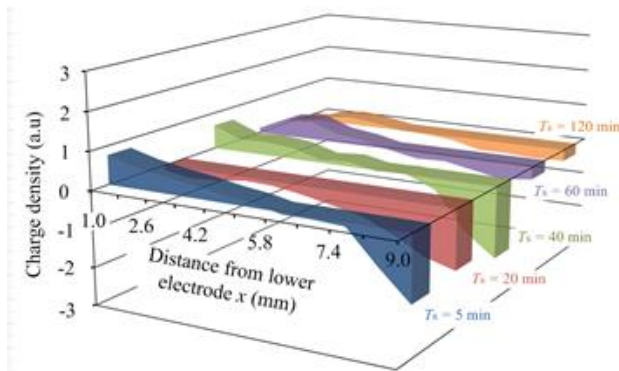


**Figure 7** Time variation of space charge density distribution for second sequence

At  $T_s = 40$  min and after, the charge layer generated by the remnant charges near both electrodes would have diminished with increasing  $T_s$ . In contrast, until  $T_s = 20$  min, the remnant charges might be in a state of movement during the rest time because the shape of charge distribution changed. If this measurement is carried out at shorter intervals of  $T_s$ , we can expect to obtain more details, regarding the space charge and the field distributions (for example, the behavior of the remnant charges during the rest time).

#### 4.0 CONCLUSION

When the voltage of  $-10$  kV and  $800$  ms was applied to the parallel plane electrode system, the measurement of the electric field distribution was carried out every  $20$  ms. Immediately after the application of the voltage pulse, the electric field distribution showed a static electric field. After several tens of milli-seconds, the electric field strength reduced due to the drop in the applied voltage. At the positions near the upper electrode, the electric field strength was very small, and the position at which the strength was

least shifted with increasing time periods. We speculated that a layer of charge might have formed in the gap. To verify this speculation, the space charge distribution was calculated by a difference method. Our results suggested that the time variation of the space charge distribution can be measured, and that electrical conduction in liquids can be studied by the evaluation of such a distribution. Moreover, using the map of the distribution, the carrier mobility in the liquid could be evaluated. In the liquid containing the charge, though the amount of charge could not be measured, the charge amount could be varied by varying the rest time. The electric field distribution was influenced by the amount of the remnant charges. Further experiments are required to study the behavior of the remnant charges.

#### Acknowledgement

This work was supported by a JSPS KAKENHI Grant (Number 2256027).

#### References

- [1] P. B. McGrath and R. W. Bradish. 1988. Optical Field Determination in Water. *IEEE Trans. EI*. 23(2): 189–195.
- [2] T. Maeno, Y. Nonaka and T. Takada. 1990. Determination of Electric Field Distribution in Oil using the Kerr-effect Technique after Application of dc Voltage. *IEEE. Trans. EI*. 25: 475–480.
- [3] U. Gäfvert, A. Jaksts, C. Törnkvist and L. Walfridsson. 1992. Electrical Field Distribution in Transformer Oil. *IEEE Trans. EI*. 27(3): 647–660.
- [4] A. Üstüindg, T. J. Gung and M. Zahn. 1998. Electro-Optic Theory and Measurements of Electric Fields with Magnitude and Direction Varying along the Light Path. *IEEE. Trans. Dielectrics EI*. 5(3): 421–441.
- [5] R. Shimizu, M. Matsuoka, K. Kato, N. Hayakawa, M. Hikita and H. Okubo. 1996. Development of Kerr Electro-optic 3-d Electric Field Measuring Technique and its Experimental Verification. *IEEE Trans. Dielectrics EI*. 3(2): 191–196.
- [6] H. Ihori, S. Uto, and K. Arii. 1996. Electrooptic Measurement of Three-Dimensional Nonuniform Electric Field Mapping in Nitrobenzene. *Jpn. J. Appl. Phys.* 35: 4550–4555.
- [7] H. Ihori, M. Fujii, and K. Arii. 1999. Measurement of Nonsymmetrical Electric Field Vector Distribution in Nitrobenzene Using Electrooptic Method. *Jpn. J. Appl. Phys.* 38: 6170–6171.
- [8] H. Ihori, M. Ujike, K. Hiromoto, M. Fujii and K. Arii. 2002. Time Series Measurements of Electric Field Vector Mapping in a Dielectric Liquid. *Jpn. J. Appl. Phys.* 41: L861–L863.